

RESEARCH ON CRACK GROWTH OF MULTIPLE-SITE DAMAGED STRUCTURE

Yuting He*, Teng Zhang*, and Ronghong Cui*

*Air Force Engineering University, China

hyt666@tom.com; zt_gm@126.com; crh-1982@163.com

Keywords: *multiple-site damage, stress intensity factor, crack growth rate, life prediction*

Abstract

Multiple-site damage (MSD) is one of the most important factors which affect structural integrity of aircrafts. In this paper, a method of MSD crack growth prediction is presented and the MSD crack growth behavior is studied. Staggered riveted lap-joint specimens were designed to simulate the actual structural details and fatigue tests were made under constant amplitude load. Stress intensity factors (SIFs) on different sides of crack tip were calculated by finite element analysis (FEA) which considering the features of bending, pin-load and friction contact. Moreover, crack growth curves were predicted by Paris formula using interval-by-interval method. The comparison of test and analyses results shows a good agreement. Using the presented method, three possible MSD modes were analyzed. Analyses results show that the crack interaction can speed up the growth rate of cracks significantly; crack growth life of MSD structure is highly conducted by leading crack and the adjacent MSD crack.

1 Introduction

The foremost technical challenge related to aging aircraft is the problem of widespread fatigue damage (WFD) [1]. Multiple-site damage (MSD) is one of the source of WFD (the other one is multiple-element damage), which characterized by the simultaneous presence of fatigue cracks in the same structural element [2]. Compared with the case of a single crack, MSD is much more dangerous to structure for it degrades the airframe residual

strength dramatically, reduces the critical crack size, and shortens the crack propagation life remarkably.

Extensive research has been carried out on MSD since the accident of Aloha 737 on 28 April 1988. In order to establish the MSD analysis guidelines and methods, many investigations have been dedicated to cracks propagation and residual strength in MSD structures. In the research field of crack propagation, much work has been performed on how to calculate stress intensity factors (SIFs) of MSD cracks and how cracks interact at the same structural element.

Exactitude calculation on MSD crack tips' SIF is the basis of crack growth analysis. Min Liao [3] has presented advanced damage tolerance analysis to support the Canadian Forces aircraft structural life cycle management, the method include new closed-form solutions and generic finite element based tools to calculate the SIF and the β -solutions for build-up structural configurations. Mayville R A [4] has studied the experiment of lap-joint and single-row-hole specimen with MSD cracks, he indicated that the analysis of lap-joint can be simplified into single-row-hole specimen, which is presented in Fig.1. Many investigators [5-8] have calculated MSD crack tips' SIF in plate specimen through analytical method or finite element method (FEM).

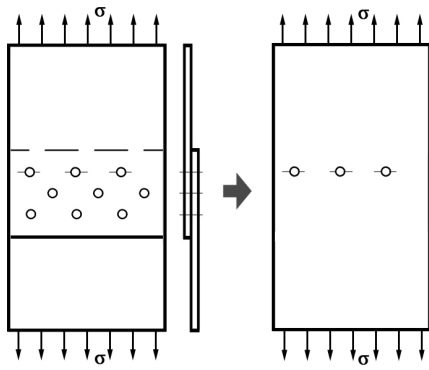


Fig. 1 Simplification of lap-joint

The interaction of multiple cracks increases the complicity of structural analysis. It is widely believed [9,10] that Paris formula, Forman formula, Willenborg formula etc. can be used to estimate crack propagation based on the solution of SIF. Fengxian Ji [11] has established an analysis method for MSD crack growth based on linear-elastic-fracture mechanics, in which SIF combination model, crack link-up criterion, fracture criterion and coherence treatment in MSD evolution are interacted.

Actually, most of the MSD cracks initiated from structures with pin-load, bending and frictional contact. Although much research has been done on MSD cracks propagation, little attention has been paid to three-dimensional (3D) lapped structures with MSD cracks. Some researchers [12,13] modeled riveted lap-joints with MSD by finite element software FRANC2D/L, but all of the models ignored the difference between K_f and K_b . As shown in Fig.2, K_f refers to the SIF of a crack tip on the front side and K_b refers to the SIF on the back side.

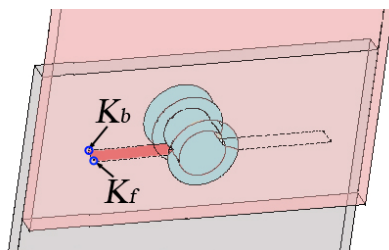


Fig. 2 Crack tips in riveted lap-joint

In this paper, fatigue tests and finite element analysis for specimens with pin-load, bending and frictional contact have been carried out to investigate the solution method for SIF

and the prediction method for MSD crack propagation; furthermore, the influence of MSD on crack growth behavior has been studied.

2 Experiments

An important aim of this paper is to establish a method to predict MSD cracks growth through finite element method. Computational tools must be verified and validated using experimental data to ensure successful transfer of useable and accurate method to application, so fatigue tests were made by MTS-810-500kN at room temperature, just as shown in Fig.3.



Fig. 3 Fatigue test

2.1 Specimen and Fixture Design

The specimens to simulate details of skins' connection in airframe are made by two types of materials. Panels are made by aluminum alloy 2524-T3 and rivets are made by titanium alloy TC4. The configuration and size of specimen is shown in Fig.4. All specimens were not pre-cracked and countersunk rivets are neatly fitted into holes.

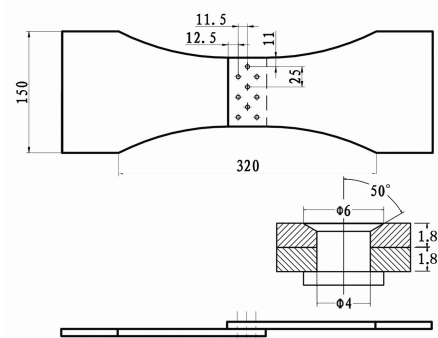


Fig.4 Staggered riveted lap-joint specimen(mm)

For typical airframe structures, skins are braced by stringers. For the purpose of simulating the actual force condition and preventing premature failure of specimen, anti-bend fixtures were designed as shown in Fig.5. The anti-bend fixture I and II are designed to prevent out-of-plane bending and the function of shims is to ensure specimen loaded in the same plane. In order to reduce the friction between specimens and fixtures during the experiment, some effective measures were taken such as inject lubricant oil or insert plastic films between contact surfaces.

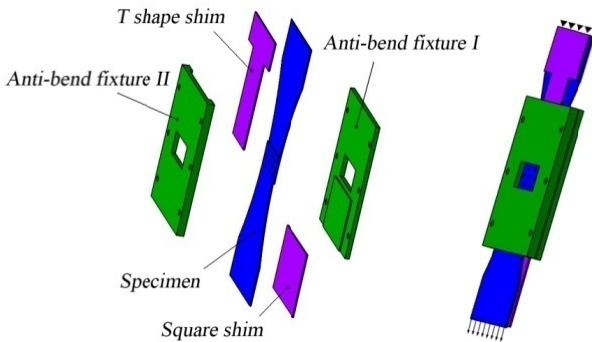


Fig. 5 Configuration of anti-bend fixtures

2.2 Test Load

All specimens were subjected to constant amplitude load; the maximum load $F_{max}=20kN$, the stress ratio $R=0$ and the load frequency $f=10$. During the entire experiment period, cracks initiation was recorded and all crack lengths were visually measured at every load increment via a traveling optical microscope.

2.3 Test Results

Three damage modes of specimens are shown in Fig.6, all of the cracks initiate and propagate in the line of the first row of rivets. There are two specimens damaged as mode one, three ones as mode two and five ones as mode three. According to experimental results, sites and sequence of crack initiation are presented in the cross section of the first row of rivets in Fig.7.

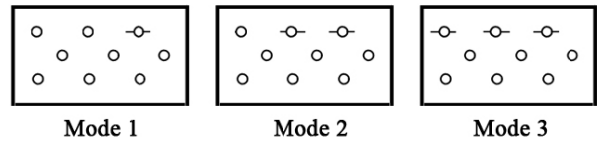


Fig. 6 Three modes of specimen damage

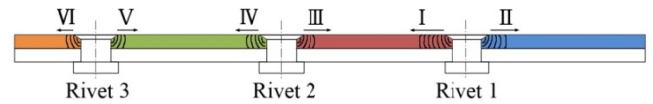


Fig.7 Sites and sequence of crack initiate

Fatigue lives of the specimens varied widely: cycle counts from 30,000 to more than 100,000. In general, specimens damaged as mode1 have longer fatigue lives than those damaged as mode2 and mode3. Since crack growth rate increased by the influence of MSD in mode2 and mode3, specimens damaged as mode1 has a longer life.

Based on the test data, it is concluded that at the initial stage of crack growth, cracks are mainly influenced by the stress concentration of holes and the interference effects between cracks are weak. When cracks extend to a certain length, the interference effects between cracks enlarge obviously along with the decrease of ligament length.

Take a specimen which damaged under mode two (Fig.8) for example, crack 1 grows independently and crack 2 is affected by crack 3. At the initial stage, the growth rates of crack 2 and crack 1 are nearly the same. As cracks grow, the ligament length between crack 2 and crack 3 decreases, growth rate of crack 2 is increased obviously, just as shown in Fig.9.



Fig. 8 Distribution of cracks

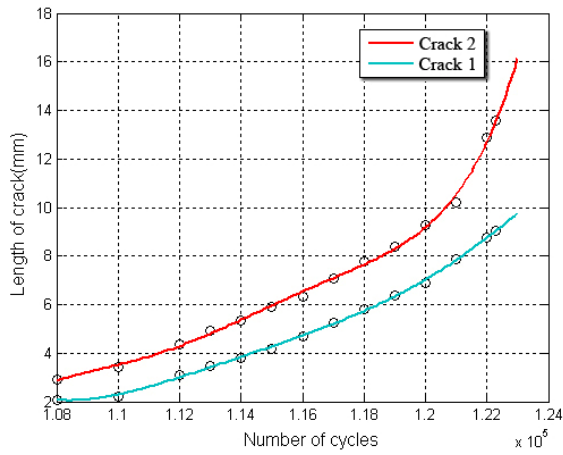


Fig. 9 Crack growth curves of crack 2 and crack 1

3 FEM and Fatigue Crack Growth Model

Accurate SIF solutions for MSD cracks at rivet holes in riveted lap-joints are difficult to determine, mainly due to the geometric complexity along with the variations in rivet load transfer, especially the interaction of MSD cracks. In this part, the FEA and interval-by-interval calculation are employed to make a simulating calculation with through-thickness cracked models under tensile load, and two growth curves of each crack have been drawn base on K_f and K_b ; furthermore, the prediction curves of crack growth are determined.

3.1 Finite Element Method

Three-dimensional finite element models are created by PATRAN as shown in Fig.10. In this figure, the full scale joint is modeled considering the features of out-of-plane bending, pin-load and friction contact. What's more, six cracks are modeled to simulate damage under mode three.

First, the global models are generated using PATRAN as a preprocessor. Using the parent model, a series of NASTRAN input files are created: each contains different cracks length, along the critical fastener row. Solid element is used for panels and the material has a Young's modulus of 72GPa, a Poisson's ratio of 0.3; meanwhile, beam element is used for rivets

which have a Young's modulus of 115GPa and a Poisson's ratio of 0.33.

1/4 Singular element is used to simulate the stress field around crack tip (Fig.10). All the possible contact areas are modeled. The rivets are modeled as 'neat fit' between holes and plates. The surface of model has the same displacement restriction and load condition as the test panels for the best boundary condition approximation.

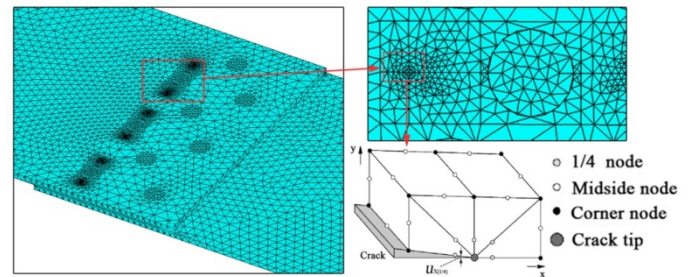


Fig. 10 Finite element model of the MSD lapped-joint

The NASTRAN static linear elastic solution was used to analyze the model. The stress analysis of model without crack shows an excellent agreement between the highest stress concentration and the experimentally observed crack initiation locations. The J-integral is utilized to calculate the K_f and K_b of crack tips.

3.2 Analytical Model for Crack Growth

Under the constant amplitude load spectrum, the crack growth was predicted by Paris formula, which is expressed as,

$$\frac{da}{dN} = C(\Delta K)^m \quad (1)$$

where,

$\frac{da}{dN}$: Crack growth rate

ΔK : Amplitude of SIF

C, m : Material related constants.

In order to realize the crack growth prediction, the base line of fatigue crack rate has to be determined. A number of tests have been performed using the middle-cracked tension (M(T)) specimens with a size of 100×300×1.8mm. The test is performed at a maximum stress of 130MPa and a stress ratio of R=0. The test crack growth rate has been fitted into Paris relation with the coefficient of crack

growth rate $C=1.6 \times 10^{-7}$ and a slope of $m=2.46$ in the dimension of $MPa\sqrt{m}$ for the SIF and mm/cycle for the crack growth rate.

The Paris crack growth model was adopted in interval-by-interval calculation and the interaction between cracks was considered by each cycle interval. This section shows the procedures that have been used to analyze the crack growth. The analysis steps are outlined below.

1. Determine damage mode.

2. Determine initial crack sizes (a_{n1}) refer to detection level or experience, where subscript n refers to ordinal number of cracks.

3. Obtain K_{nf} and K_{nb} of crack tips by FEM; because $R=0$, ΔK_{nf} and ΔK_{nb} can be confirmed.

4. Set cycle interval (ΔN_i). In this paper, set $\Delta N=2000$ when the ligament length above half distance of the holes, and set $\Delta N=500$ when the ligament length below half distance of the holes. The interaction between cracks is considered invariable in each cycle interval.

5. Base on Paris formula, Δa_{ni} can be calculated as,

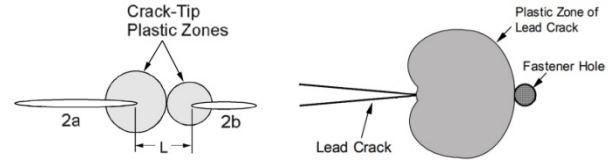
$$\Delta a_{ni} = \begin{cases} \Delta N_i \times C(\Delta K_n)^m + a_{ni} & (i = 1) \\ [2 \times C(\Delta K_n)^m - \frac{\Delta a_{n(i-1)}}{\Delta N_{(i-1)}}] \times \Delta N_i + a_{ni} & (i > 1) \end{cases} \quad (2)$$

6. Set $a_{n(i+1)} = a_{ni} + \Delta a_{ni}$; next, return to step3 and continue calculation.

The circulation from step3 to step6 will stop when the specimen is destruct. Failure criterion is shown as Fig.11. When the leading crack and the smaller crack will coalesce when their plastic zones come into contact with each other (Fig.11 (a)) or the plastic zone of leading crack will contact a nearby fastener hole(Fig.11 (b)), conclusion can be made that the whole structure will destruct[2]. Irwin model was used to estimate a crack tip plastic zone size, which is expressed as,

$$r_p = \frac{1}{2\pi} \left(\frac{K_I}{F_{TY}} \right)^2 \quad (3)$$

where, r_p , K_I and F_{TY} are the plastic zone size, crack tip SIF and yield strength respectively.



(a) With MSD (b) Without MSD

Fig. 11 Illustration of the Plastic Zone Linkup (PZL) Criterion

After calculation, two crack growth curves of each crack tip can be obtained base on K_f and K_b .

3.3 Crack Growth Curve

Take a specimen damaged under mode three for example, the experimental crack growth curves and the curves drawn by K_f and K_b is plotted in Fig. 12. Different from the former method, the initial crack sizes are determined by experimental data.

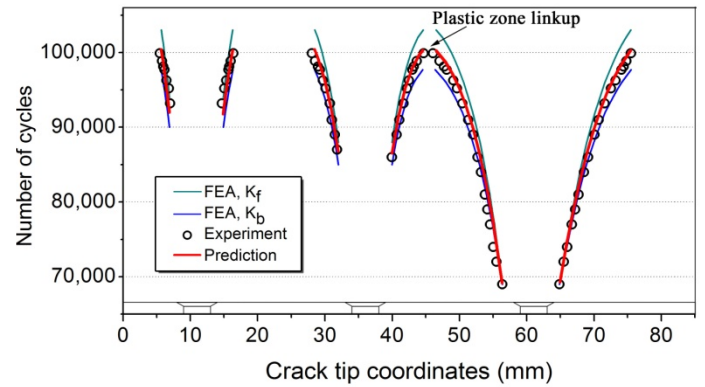


Fig. 12 Comparison of predicted and experimental curves

The figure shows that the experimental crack growth curves lay in the middle of the two curves drawn by K_f and K_b . So, the medium line of two curves can serve as the prediction curve of crack growth.

3.4 Comparison of 3D and 2D FEA

In order to compare the presented method and the method mentioned in literature [4], 3D and 2D finite element models are established by PATRAN as shown in Fig.13. The models are damaged under model1.

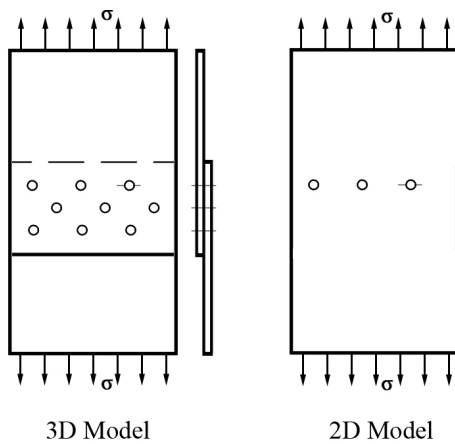


Fig. 13 3D and 2D models

SIFs are calculated by NASTRAN and crack growth predicted curves are drawn by interval-by-interval calculation, just as shown in Fig.14.

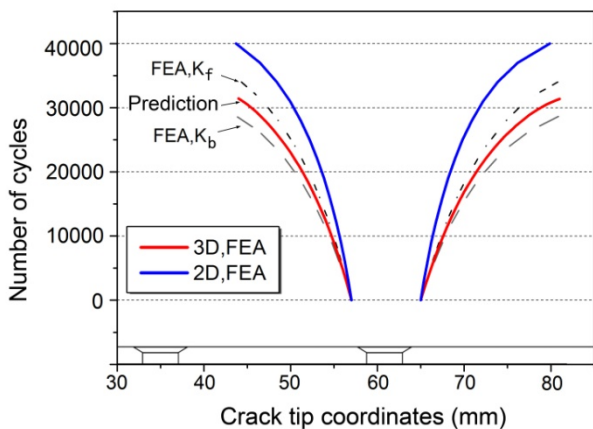


Fig. 14 Comparison of 3D and 2D FEA

It can be seen from this figure that the crack growth cycles predicted by 2D FEA are about 30% higher than those by 3D FEA. Compared with 3D FEA, the result of 2D FEA is much more dangerous for life prediction.

4 Prediction of Crack Growth

According to experimental results, three initial damaged modes and crack ordinal numbers are defined as shown in Fig.15. The initial length of leading cracks (crack1 and crack 2) is 2mm, and the initial length of MSD cracks (crack 3 to crack 6) is 1mm.

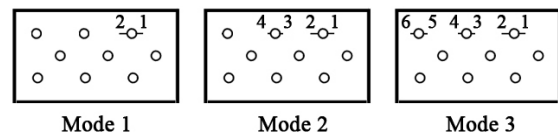


Fig. 15 Three initial damaged modes

4.1 Crack Growth Curves

Use the method presented in Section 3.2, crack growth curves from initial to failure under three models are predicted. Fig.16 shows the crack growth curves under three modes. Compared with non-MSD mode (mode1), the crack growth lives of MSD modes (mode2 and mode3) are about 50% shorter; we can conclude that crack interaction can speed up the expansion of cracks significantly.

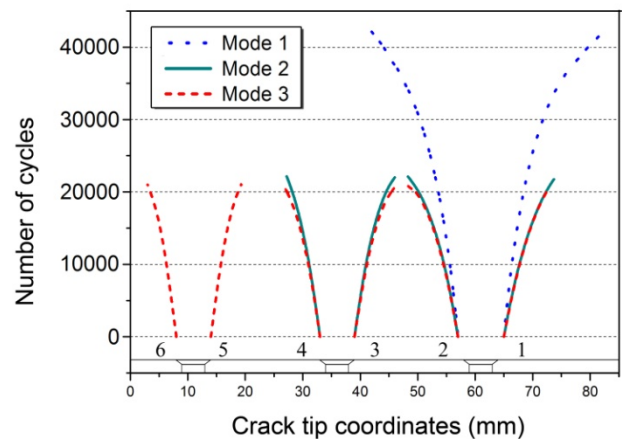


Fig. 16 Crack growth curves under three modes

At the initial stage of crack growth, crack1 to crack4 of mode2 and mode3 are overlapped. Branches appear when cracks extend near to critical length. In general, the crack growth lives of mode2 and mode3 has a little difference, which indicates that the appearance of crack5 and crack6 has little affection on crack growth life. It can be deduced that the crack growth life of MSD structures is highly conducted by the leading crack and the adjacent MSD crack.

4.2 Crack Growth Rate Curves

Crack growth rate is approximately determined as $\Delta a/\Delta N$, Fig. 17 shows the crack growth rate curves from initiation to failure under three modes.

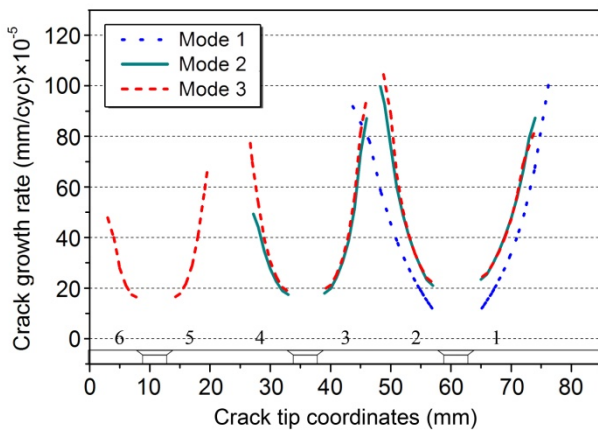


Fig. 17 Crack growth rate curves under three modes

From Fig.17, some significant conclusions are obtained as follows.

1. At the same length, the crack growth rate of multiple cracks is much bigger than that of single crack.

2. At the initial stage of crack propagation, cracks initiated from one hole have the same growth rate; cracks are mainly influenced by the stress concentration of holes and the interference effects between cracks are weak.

3. At the end stage of crack propagation, the interference effects between cracks enlarged obviously with the decrement of ligament lengths, which are in agreement with the test results.

4. Comparing mode3 with mode2, the growth rate of crack4 is greatly affected by the appearance of crack5 and crack6, while the grow rates of others remain almost no change. Crack growth rate is susceptible to adjacent crack rather than non-adjacent crack.

5 Conclusions

Much work has been done in the research field of MSD crack propagation, and a lot of methods were developed to calculate the SIF of MSD crack tips. However, most of the studies were carried out on the basis of plane structure. These studies neglected the effect of complicated stress state in actual structures, and the difference between SIFs on different sides of the crack tip is ignored.

In this paper, fatigue tests and finite element analysis for specimens considering

pin-load, bending and frictional contact have been carried out; a life prediction method has been developed depend on the calculation of K_f and K_b . The comparison of test and analyses results shows that the prediction method is practical. Furthermore, three possible MSD modes were analyzed by the presented method. The results of this study may provide reference for MSD tolerance analysis.

However, some limitations in this paper are worth noting. The analysis model is too small to represent actual structures and the calculation process is too complex to use in large-scale analysis. Future work should therefore include full-scale model analysis and convenient method research.

Acknowledgements

Thanks to the First Aircraft Institute of Aviation Industry Corporation of China for computational support.

References

- [1] DAVID Y.JEONG and PIN TONG. Onset of multiple site damage and widespread fatigue damage in aging airplanes. *International Journal of Fracture*, Vol. 85, pp 185-200, 1997.
- [2] Swift T. Widespread fatigue damage monitoring-issues and concerns. *Proceedings of the 5th International Conference on Structural Airworthiness of New and Aging Aircraft*, Germany, pp133-150, 1993.
- [3] Liao Min, Yan Bombardier and Guillaume Renaud. Advanced damage tolerance and risk assessment methodology and tool for aircraft structures containing MSD/MED. *The 27th International Congress of the Aeronautical Sciences*, France, 2010.
- [4] Mayville R A, Warren T J. A laboratory study of fracture in presence of lap s plice multiple site damage. *Atluri S N, Sampath S G, Tong P Eds, Structural integrity of aging airplanes*, Berlin Heidelberg, pp 263- 273, 1991.
- [5] Shuxiang Guo, Xiwu Xu. A study on the stress intensity factors of a finite plate with multiple elliptical holes and cracks. *ACTA MECHANICA SOLIDA SINICA*, Vol.26, No.3, pp 351-358, 2005.
- [6] YU Dazhao, CHEN Yueliang , YU Zhangyan. Finite element analysis of SIF of flat MSD panels with a number of collinear holes. *JOURNAL OF NAVAL AERONAUTICAL ENGINEERING INSTITUTE*, Vol.21, No.2, pp 561-565, 2006.

- [7] Xue Xiaofeng, Feng Yunwen, Ying Zhongwei. Research on the plant multiple cracks stress intensity factors based on stochastic finite element method. *Chinese Journal of Aeronautics*, Vol.22, pp 257-261, 2009.
- [8] Park JH, Atluri SN. Analysis of a cracked thin isotropic plate subjected to bending moment by using FEAM. *KSME International Journal*, Vol.13, pp 912-917, 1999.
- [9] Ren Keliang, Lu Guozhi. Fatigue propagation analysis of three-dimensional widespread cracks. *ACTA AERONAUTICA ET ASTRONAUTICA SINICA*, Vol.30, No.3, pp 462-467, 2009.
- [10] NIE Xuezhou, WANG Zhizhi and CHEN Li. Test verification approach of stress intensity factor for multiple site cracks of stiffened panel. *Chinese Journal of Mechanical Strength*, Vol.26, No.S, pp 301-303, 2004.
- [11] JI Fengxian, XU Xiaofei and YAO Weixing. Study on analysis method of multiple site damage fatigue crack growth. *Chinese Journal of Mechanical Strength*, Vol.25, No.3, pp 264-266, 2003.
- [12] CHEN Yue-liang, YU Da-zhao, YANG Mao-sheng. Finite element analysis of stress intensity factors of lap joint with multiple site damage. *ACTA AERONAUTICA ET ASTRONAUTICA SINICA*, Vol.28, No.3, pp 615-619, 2007.
- [13] Brett L, Ching-Long Hsu, Patricia J. Evaluation and verification of advanced methods to assess multiple-site damage of aircraft structure, DOT/FAA/AR-04/42,1, 2004.

Copyright Statement

The authors confirm that they, and/or their company or organization, hold copyright on all of the original material included in this paper. The authors also confirm that they have obtained permission, from the copyright holder of any third party material included in this paper, to publish it as part of their paper. The authors confirm that they give permission, or have obtained permission from the copyright holder of this paper, for the publication and distribution of this paper as part of the ICAS2012 proceedings or as individual off-prints from the proceedings.